



Received on 16 August 2022; received in revised form, 25 September 2022; accepted 20 November 2022; published 01 April 2023

## COMPUTER-BASED SCREENING OF THE ANTICANCER PROPERTY OF SELECTED PANAX GINSENG PHYTO-LIGANDS

Ezekiel A. Olugbogi<sup>\* 1,2</sup>, Olaposi I. Omotuyi<sup>1,5</sup>, Kolawole T. Mesileya<sup>1,5</sup>, Damilola S. Bodun<sup>1,2</sup>, Shola D. Omoseeye<sup>1,4</sup>, Anita O. Onoriode<sup>1</sup>, Favour O. Oluwamroti<sup>1,3</sup>, Joshua F. Adedara<sup>1,3</sup>, Isaac A. Oriyomi<sup>1,3</sup>, Fatimat O. Bello<sup>1,4</sup>, Favour O. Olowoyeye<sup>1,3</sup>, Oluwatomilola G. Laoye<sup>1,2</sup>, Damilola B. Adebowale<sup>1,2</sup>, Aanuoluwapo D. Adebisi<sup>1</sup>, Mark-Solomon C. Ogologo<sup>1,5</sup>, Obinna C. Etukokwu<sup>1,5</sup>, Ifeanyichukwu O. Onyemaobi<sup>1,5</sup>, Salim Y. Jibril<sup>1,5</sup> and Precious C. Onyeka<sup>1,5</sup>

Molecular Biology and Simulation Center<sup>1</sup>, Ado-Ekiti, Ekiti State, Nigeria.

Department of Biochemistry<sup>2</sup>, Adekunle Ajasin University, Akungba-Akoko, Ondo State, Nigeria.

Department of Physiology<sup>3</sup>, Ekiti State University, Ado-Ekiti, Ekiti State, Nigeria.

Department of Anatomy<sup>4</sup>, Ekiti State University, Ado-Ekiti, Ekiti State, Nigeria.

College of Pharmacy Afe Babalola University<sup>5</sup>, Ado-Ekiti, Ekiti State, Nigeria.

### Keywords:

Cancer, Phyto-ligand, Pharmacokinetics, Panax Ginseng, Glucose Transporter 4 (GLUT-4), *In-silico* and Density functional theory (DFT)

### Correspondence to Author:

**Olugbogi Ezekiel Abiola**

Molecular Biology and Simulation Center, Ado-Ekiti, Ekiti State, Nigeria.

**E-mail:** olugbogiezekiel@gmail.com

**ABSTRACT:** It cannot be overstated that the rate at which cancer uses glucose for proliferation is one of the many variables contributing to the alarmingly high mortality rate of cancer over time. Cancerous cells can survive because of this. However, a significant therapeutic strategy for malignant cells may involve the blockage of several glucose transporters, including glut 4 encoded by the solute carrier family-2-member-4-gene (Slc2a4) by certain phytochemicals from Panax ginseng. The top ten phytochemicals obtained from the PubChem database in SDF format with the lowest binding energies of these compounds with SGLUT4 were selected as possible inhibitors of GLUT4 from Panax. Glut 4 complexed with cytochalasin B was retrieved from the protein data bank (Rcsb.pdb). Schrodinger, online tools such as ProTOX, swissAdmet and Spartan 10.1 were used to examine the samples' Mmgbsa, Admet characteristics, drug-likeness, toxicity prediction and DFT. The results of this *in-silico* study showed that the docking scores of the 10 compounds were higher than those of the co-crystallized compound. The Lipinski rule of five (RO5) and the ADMET property revealed that seven out of ten compounds did not violate any of the rule's requirements for oral drug ability, while two compounds did so. Quercetin, however, was discovered to have a higher docking score than Cytochalasin B and to have broken no rules of the RO5. These *in-vitro* investigations suggest that Quercetin, in particular, could be a strong therapeutic agent with greater therapeutic efficacy than Cytochalasin B in the therapy of cancer by inhibiting GLUT4.

**INTRODUCTION:** With a record of about ten million fatalities in the year 2020<sup>1</sup> and ranking as the second most common cause of death in many

nations, cancer is a disease with some components that makes finding a solution nearly hard.

Problems, such as the different elements that cause it and the fact that these factors do not express themselves in each cause of cancer with a uniform pathway across all cancer types are confronted in the search for a solution to cancer<sup>2</sup>. However, a select few variables are mostly responsible for cancer. These elements have been tracked and found to play a role in the development of several

	<p style="text-align: center;"><b>DOI:</b> 10.13040/IJPSR.0975-8232.14(3).1714-27</p>
	<p style="text-align: center;">This article can be accessed online on <a href="http://www.ijpsr.com">www.ijpsr.com</a></p>
<p>DOI link: <a href="https://doi.org/10.13040/IJPSR.0975-8232.14(3).1714-27">https://doi.org/10.13040/IJPSR.0975-8232.14(3).1714-27</a></p>	

cancer types. The most common reasons include genetic mutation, lifestyle and food, radiation, and hormonal variables. Fundamentally, cancer is brought on by genetic alteration. Cancer is a hereditary illness that is brought on by a combination of internal genetic problems and exposure to environmental stimuli. When DNA is exposed to carcinogenic substances, the sickness starts at the cellular level and finally changes DNA<sup>3</sup>.

Some substances can cause cancer and mutation in the meals we eat. However, studies have shown that eating plenty of fruits and vegetables can lower your risk of developing cancer, especially since these plants have been found to contain some anti-cancer components. You can also lower your risk of developing cancer by staying physically active and maintaining a healthy weight<sup>4, 5, 6</sup>.

Red meat, dairy milk, salted, smoked foods, alcohol, and processed milk have all been identified as indicators of cancer<sup>6</sup>. Breast cancer, for example, is mostly brought on by hormonal imbalance<sup>7</sup>. Early menstruation, late menopause, puberty-related obesity, high estrogen levels in postmenopausal women and not breastfeeding are all examples of hormonal imbalances that increase women's chances of developing cancer<sup>8, 9, 10, 11, 12, 13</sup>.

Certain therapeutic options have been developed over the years of this life-threatening disease. A clinically proven medication for managing and treating cancer is metformin. Numerous statistical findings have supported this claim. Metformin prevents malignant cells from proliferating and multiplying. There are two known pathways by which it operates: either by the I/IGF pathway, which inhibits the growth of cancer by reducing I/IGF-1 in the blood, which inactivates its downstream signaling pathway, or by the AMPK pathway, which enables the common drug metformin to act directly on cancer cells by raising AMPK levels and inhibiting mTOR<sup>14, 15</sup>.

Another common treatment for this disease is chemotherapy, however, because of its numerous negative effects, it is not generally advised<sup>16</sup>. The challenge in treating cancer is identifying and destroying cancer cells while overcoming drug

resistance<sup>17, 18</sup>. In response to these setbacks, a recent finding by Mohamed Yafout<sup>19</sup>, suggested that chemotherapeutics might be mounted onto gold nanoparticles because they have the precise size and surface qualities to transport the drugs to the target site.

**GLUT-4 Inhibition:** Glut-4, one of the body's 14 different types of glucose transporters, is mostly present in adipose tissues and skeletal muscle cells. It plays a role in the process by which glucose enters cells from the blood<sup>20, 21, 22</sup>.

The majority of Glut 4 transporters are found embedded inside intracellular components of the cells, but when activated, they induce Glut 4 to move to the plasma membrane, opening the possibility of glucose influx into the cells in the future<sup>23</sup>.

Glycolytic processes are substantially enhanced during the development of cancer cells, and this promotes the spread and growth of tumors in the cells<sup>24, 25, 26</sup>. Reviews demonstrate that these tumors have significantly elevated levels of glut 1 and glut 4. Insulin signaling is crucial for glut 4 translocation to the plasma membrane.

In cancer chemotherapy, glucose transporter 4 (GLUT-4) inhibitors and antagonists are employed as treatments<sup>27</sup>. Cancer cells eat more glucose to support the metabolic processes essential to their survival, development, and proliferation. The high-affinity glucose transporters GLUTs-1 and 4 are among the fourteen SLC2A family members. GLUT-4 is abundantly expressed in adipose tissue and muscles<sup>22</sup>.

**Panax Ginseng:** The genus *Panax* includes the perennial plant ginseng (*Araliaceae* family).

The genus *Panax* (*Panax quinquefolium* L.) has more than twelve distinct species of ginseng. The two most well-known species among them, Asian ginseng and American ginseng are frequently employed for their therapeutic benefits<sup>30</sup> as shown in **Fig. 1** and **Fig. 2**. In East Asia, particularly in China, Korea and Japan, Asian ginseng (*Panax ginseng*) root has been extensively used for thousands of years as an important source of natural medicine.



FIG. 1: PANAX GINSENG DISPLAYING ITS FRUIT, TREES AND ROOTS <sup>28</sup>



FIG. 2: PANAX GINSENG <sup>29</sup>

## METHODS:

**Ligands and Protein:** As previously documented in literature reviews on the plant's phytochemicals, 96 compounds were found in Panax ginseng extracts. The 2D structures of these compounds were downloaded from the online databases Pubchem and ChemDraw Ultra (RRID: SCR 016768). The ligands were docked to a Cytochalasin B and GLUT 4 complexed human crystal (PDB ID: 7WSM). A protein data bank was used to get the protein. (<http://www.rcsb.org>). The 2-Dimensional Structures of the 96 ligands were imported and prepared using the ligprep tool.

**Molecular Docking:** The computer-based drug test was conducted using Maestro 11.1 and Schrödinger Suite software <sup>31</sup>. It generated a glide grid. The docking process utilizes the HTVS (high

throughput virtual screening) and XP precisions (extra precision). The top ten ligands with the lowest docking scores were docked once again utilizing additional precision after all ligands produced from the plant Panax ginseng were docked using HTVS docking for screening (XP). The scores for docking were calculated in Kcal/mol.

**MM/GBSA:** The docked protein-ligand complex binding free energy was calculated using the Molecular Mechanics/Generalized Born Surface Area (MM/GBSA) continuum solvent model as part of the computer-based drug design process. The OPLS3 force field, the VSGB solvent model, and rotamer search methods from Prime were combined to complete this project.

**ADME Analysis:** The ADMET (Absorption, Distribution, Metabolism, Excretion and Toxicity) parameters were calculated on Maestro using the Qikprop program. ADMET we measured variables such as molecular weight, log P, Lipinski's rule of five violations, topological polar surface area, and the number of hydrogen bond acceptors and donors. ADMET pharmacological parameters clearly describe the pharmacokinetics and Pharmacodynamic profiles of therapeutic molecules.

**Density Functional Theory (DFT):** The molecular characteristics of a few Panax compounds were evaluated using quantum chemical calculation using density functional theory to anticipate the biological activities of the top-ranked compounds (DFT). After the molecules underwent a conformer distribution calculation, the most stable conformer was picked for the DFT analysis in vacuum using Spartan 10 computational chemistry software. The thermodynamic parameters, EHOMO and ELUMO were computed. The global reactivity descriptors and other characteristics were generated from the EHOMO and ELUMO values. The energy bandgap was calculated from the difference between ELUMO and EHOMO (Eg).

$$E_g = E_{LUMO} - E_{HOMO} \quad (1)$$

While Koopman's theory connects the Ionization energy (I) and Electron Affinity (A) to EHOMO and ELUMO (Koopmans, 1993).

$$I = -E_{HOMO} \quad (2)$$

## RESULTS:

**TABLE 1: ADME ANALYSIS**

Entry Name	Docking Score	XP GScore	MMGB SA dG	QP Log HERG	QPPCaco	QPlogB B	QPPMD CK	QPLOG 7Khsa	Rule of Five
Epigallocatechin galate	-14.063	-14.122	-34.471	-5.412	0.804	-4.333	0.223	-0.515	2
Ginsenoside Rh 1	-13.312	-13.312	-59.497	-4.469	55.862	-2.625	21.884	0.14	2
Myricetin	-10.042	-10.054	-47.643	-4.868	7.16	-2.853	2.375	-0.495	1
Quercetin	-9.852	-9.863	-51.274	-4.922	20.4	-2.31	7.366	-0.358	0
Catechin	-9.545	-9.545	-39.293	-4.804	53.333	-1.899	20.815	-0.426	0
Apigenin	-9.323	-9.339	-35.795	-5.088	117.104	-1.432	48.707	-0.045	0
Hesperitin	-8.719	-8.734	-54.406	-5.048	121.621	-1.531	50.74	-0.006	0
Genistein	-8.635	-8.647	-40.813	-4.909	167.424	-1.3	71.678	-0.119	0
Kaempferol	-7.961	-7.972	-46.832	-4.988	58.447	-1.78	22.981	-0.211	0
Formononetin	-7.88	-7.889	-42.158	-5.001	392.675	-0.892	180.114	-0.159	0
Cytochalasin B (co-crystallized)	-6.635	-6.635	-48.971	-3.998	190.425	-1.233	136.384	0.547	0

$$A = -E_{LUMO} \quad (3)$$

$$\chi = 1 + A / 2 \quad (4)$$

$$\eta = 1 - A / 2 \quad (5)$$

$$\delta = 1 / n \quad (6)$$

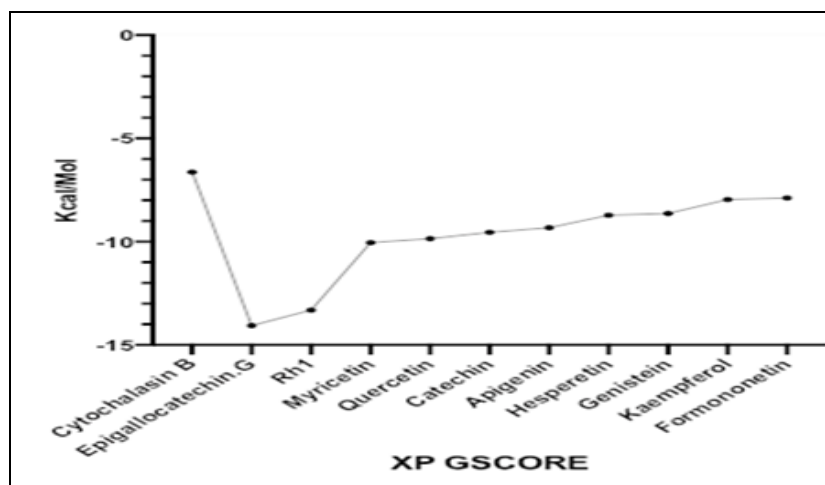
**Pharmacokinetics and Drug Likeness Analysis:** Using the first 10 compounds with the lowest docking scores retrieved from the PubChem database, a web-based tool called SwissADME (<https://www.swissadme.ch/>) and Pro-Tox (<https://tox-new.charite.de/protox-II/>) were used to test the drug likenesses potential of the compound of the plant, Panax ginseng. The isomeric grins of the compound on the PubChem database were extracted to produce the toxicity values. The isomeric smiles were then copied onto the Swiss ADME website to gather data on bioavailability, oral absorption, the gut-blood barrier, metabolic reactions, Cytochrome P450 reactions, and their capacity to penetrate the blood-brain barrier. All these are pharmacological parameters that are the general template for accessing the affinity of chemical compounds to be further developed as potential drugs.

Each toxicology parameter was predicted by pasting its isomeric grins and choosing the different particular toxicity parameters using the tox prediction option. This process is also derived from toxicology parameters such as mutagenicity, hepatotoxicity, and carcinogenicity.

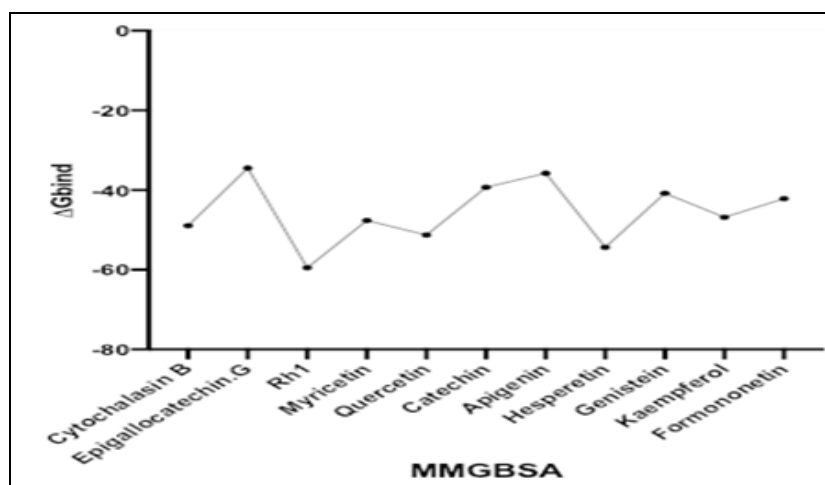


**TABLE 2: HYDROGEN BONDS AND HYDROPHOBIC INTERACTIONS OF THE HIT PHYTOCHEMICALS**

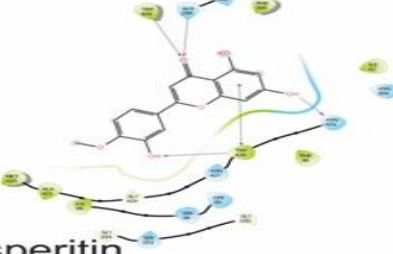
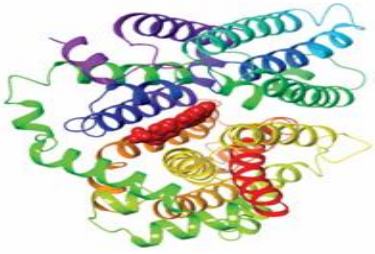
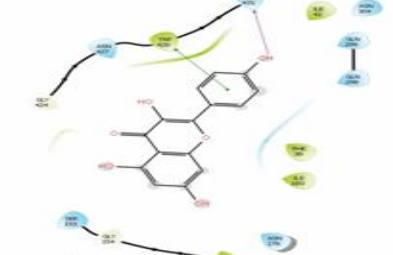
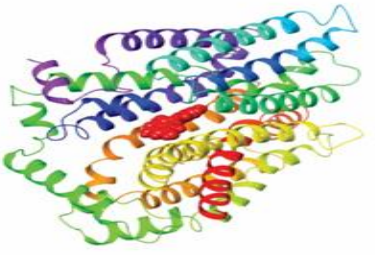
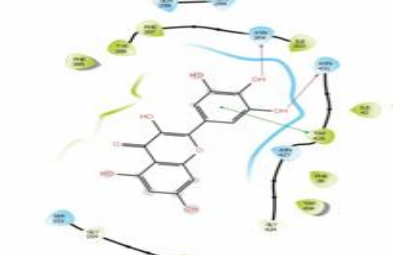

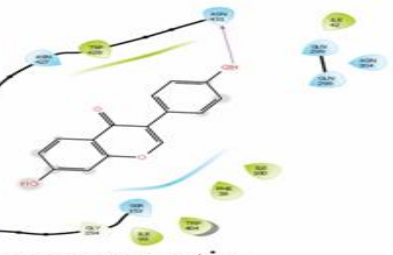
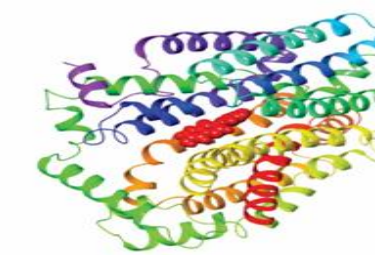
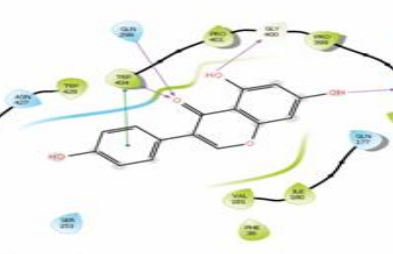
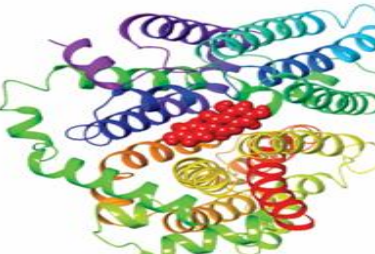
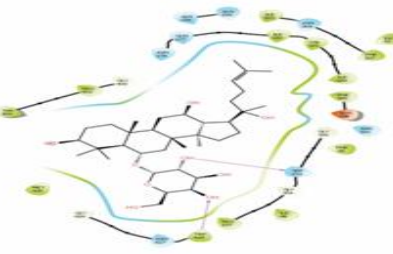
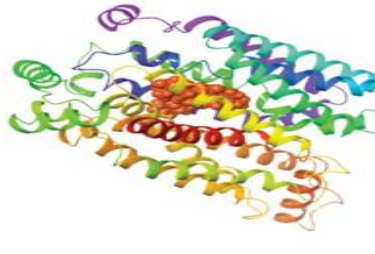
Entry Name	H-bond	Hydrophobic interacting amino acids	Other interactions
Epigallocatechin galate	NONE	PRO 165, ILE 163, PHE 29, VAL 28, ALA 27, LEU 26, VAL 25, LEU 24, LEU 247, LEU 172, PRO 224, CYS 223, PHE 222	NONE
Rh1	TRP 428, SER 153	ILE 303, ILE 42, ILE 180, VAL 181, ILE 184, PHE 395, PHE 38, PHE 307, PRO 401, TRP 404, MET 420, TRP 428, PRO 157, ILE 99	NONE
Myricetin	ASN 413, ASN 304	PHE 307, TYR 308, PHE 395, ILE 303, ILE 42, PHE 88, TRP 428, PHE 39, TRP 404, PRO 157	Pi Pi Stack: TRP 428,
Quercetin	ASN 431, ASN304, SER 153	ILE 42, PHE 307, TYR 308, ILE 180, PHE 38, TRP 428, ILE 99, PRO 157, TRP 404	Pi Pi Stack: PHE 38
Catechin	GLN 299, GLH 396	TRP 428, PHE 38, PHE 307, PHE 395, ILE 180, VAL 181, ILE 184, ILE 42	Pi Pi Stack: PHE 38
Apigenin	GLH 396, ASN 431, ASN 304	PHE 395, ILE 180, VAL 181, ILE 184, PHE 38, PHE 307, TYR 308, TRP 428, TRP 404, PRO 401.	NONE
Hesperitin	TRP 404, GLN 298, TRP 428, ASN 431	TRP 404, PHE 395, ILE 42, PHE 38, TRP 428, MET 420, ALA 421, ILE 99	Pi Pi Stack: TRP 428
Genistein	TRP 404, GLN 298, GLY 400, GLH 396	TRP 428, TRP 404, PRO 401, PRO 399, PHE 395, VAL 181, ILE 180, PHE 38	NONE
Kaempferol	ASN 431	ILE 42, TRP 428, PHE 38, ILE 180, PRO 157, TRP 404	Pi Pi Stack: ASN 431
Formononetin	ASN 431	TRP 428, ILE 42, ILE 180, PRO 157, ILE 99, TRP 404, PHE 38	NONE



**FIG. 3: XP GSCORE OF THE TOP 10 LIGANDS OF THE PLANT, PANAX GINSENG**



**FIG. 4: MMGBSA SCORES OF TOP LIGANDS WITH LOWEST DOCKING SCORE**

2D STRUCTURE	3D STRUCTURE
 <p data-bbox="289 430 483 464"><b>Hesperitin</b></p>	
 <p data-bbox="289 735 511 770"><b>Kaempferol</b></p>	
	
2D STRUCTURE	3D STRUCTURE
 <p data-bbox="289 1365 609 1386"><b>Formononetin</b></p>	
 <p data-bbox="289 1659 462 1692"><b>Genistein</b></p>	
	

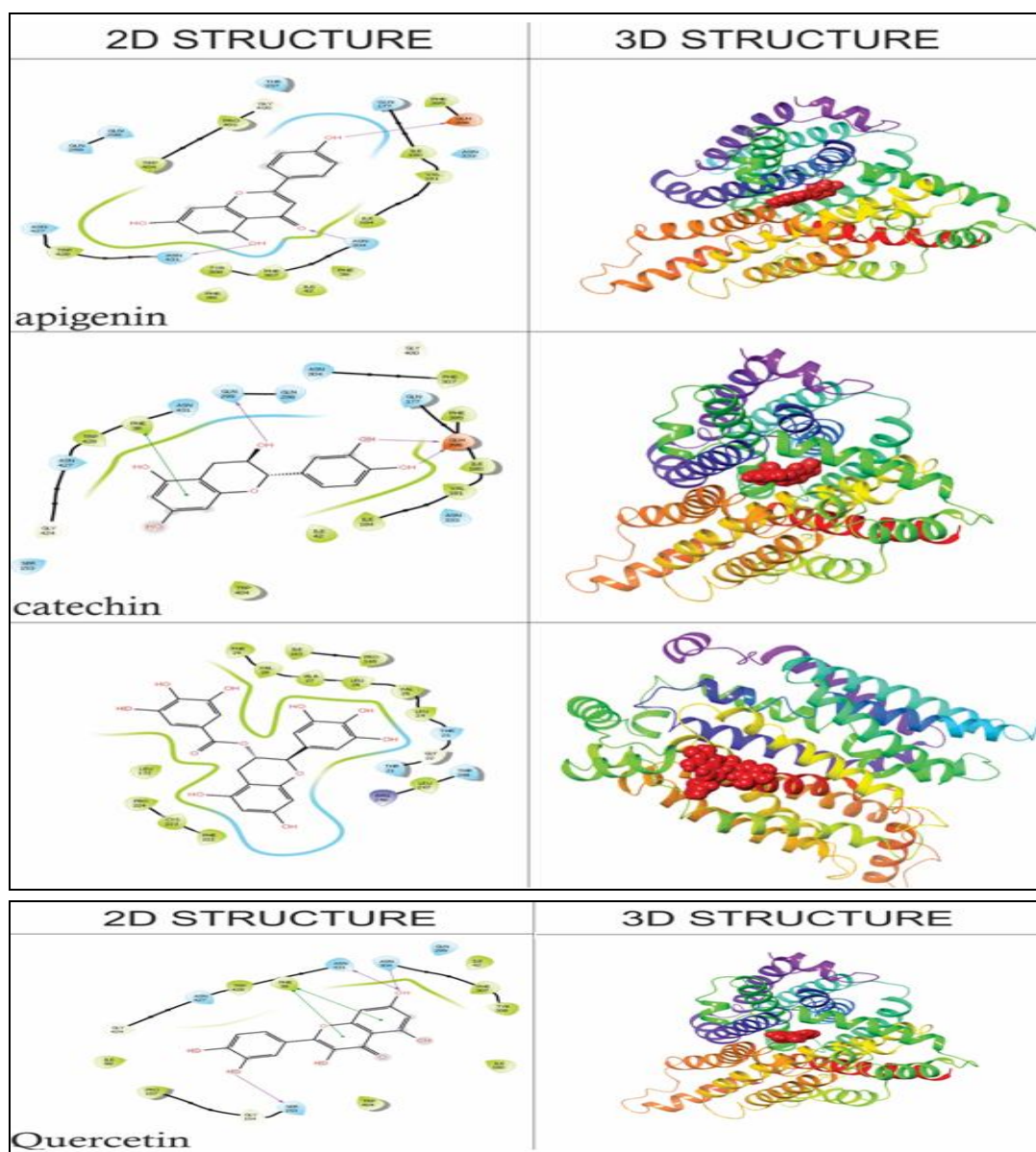


FIG. 5: 2D STRUCTURE AND 3D STRUCTURE OF TOP 10 COMPOUNDS OF THE PLANT, PANAX GINSENG

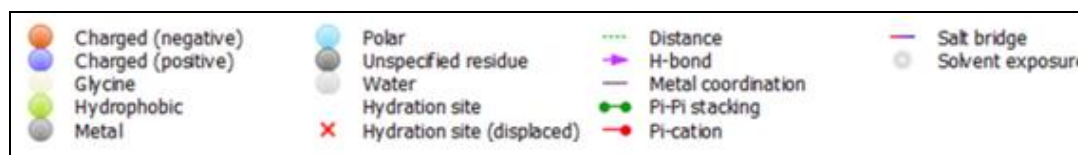


TABLE 3: *IN-SILICO* DRUG LIKENESS PREDICTION OF THE COMPOUNDS

Compounds	Molecular weight (g/mol)	Num. H bond acceptor	Num. H bond donor	TPSA (Å <sup>2</sup> )	ILOGP	Bioavailability Score	Log kP (cm/s)
Epigallocatechin galate	458.37	11	8	197.37	1.53	0.17	-8.27
Ginsenoside Rh 1	638.87	9	7	160.07	4.49	0.17	-7.17
Myricetin	318.24	8	6	151.59	1.08	0.55	-7.40
Quercetin	302.24	7	5	131.36	1.63	0.55	-7.05
Catechin	290.27	6	5	110.38	1.33	0.55	-7.82
Apigenin	270.24	5	3	90.9	1.89	0.55	-5.80
Hesperitin	302.28	6	3	96.22	2.24	0.55	-6.30
Genistein	207.24	5	3	90.80	1.91	0.55	-6.05
Kaempferol	286.24	6	4	111.13	1.70	0.55	-6.70
Formononetin	268.26	4	1	59.67	2.49	0.55	-5.95

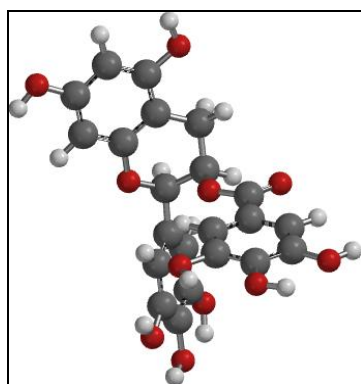


**TABLE 4: TOXICITY AND DRUG-LIKENESS PARAMETERS**

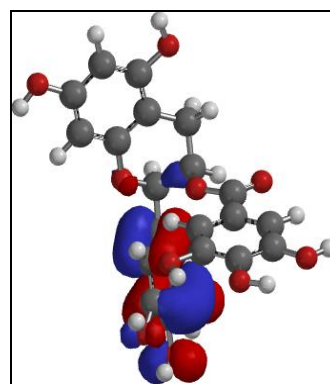
Entry Name	GI Absorption	BBB Permeant	P-gp Substrate	CYP3A4 Inhibitor	Hepatotoxicity	Carcinogenicity	Mutagenicity
Epigallocatechin gallate	Low	No	No	No	Inactive	Inactive	Inactive
Ginsenoside Rh 1	Low	No	Yes	No	Active	Inactive	Inactive
Myricetin	Low	No	No	Yes	Inactive	Active	Active
Quercetin	High	No	No	Yes	Inactive	Active	Active
Catechin	High	No	Yes	No	Active	Inactive	Active
Apigenin	High	No	No	Yes	Active	Inactive	Inactive
Hesperitin	High	No	Yes	Yes	Inactive	Inactive	Inactive
Genistein	High	No	No	Yes	Active	Inactive	Inactive
Kaempferol	High	No	No	Yes	Active	Inactive	Inactive
Formononetin	High	Yes	No	Yes	Active	Inactive	Inactive

**Compound ID**  
Epigallocatechin gallate

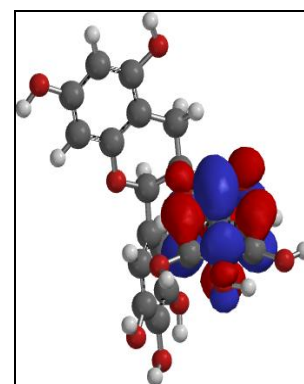
**Optimized**



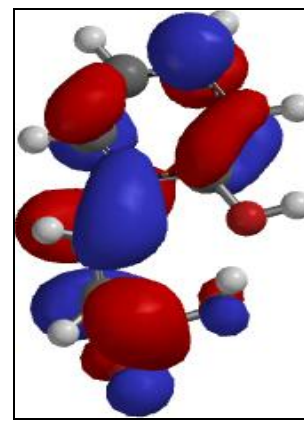
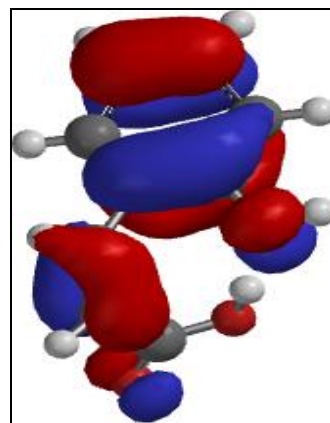
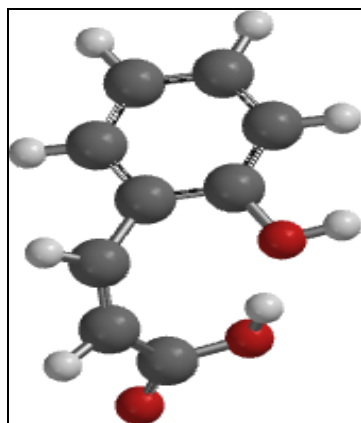
**Homo**



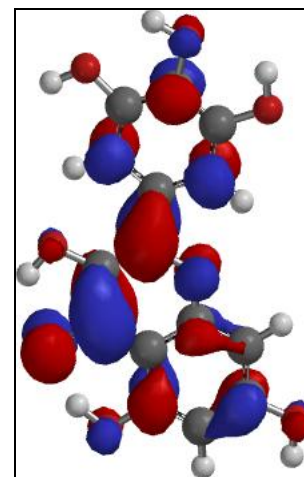
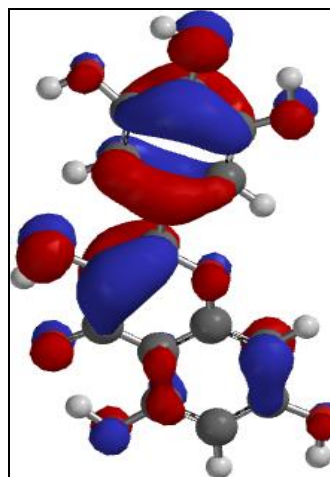
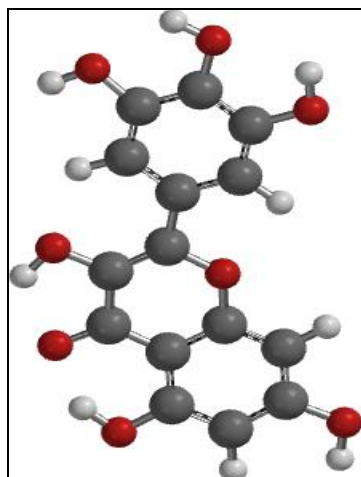
**Lumo**



**Myricetin**

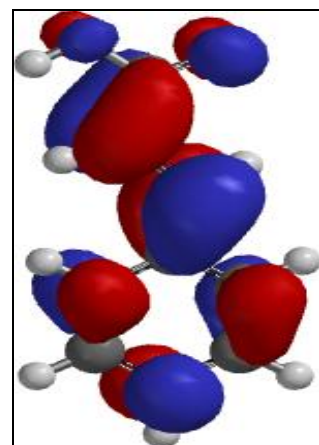
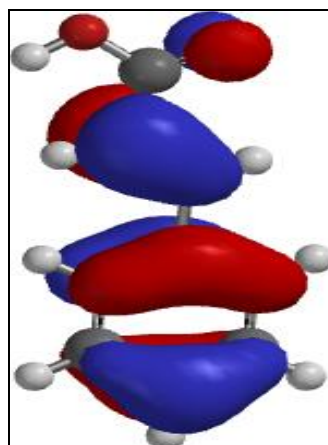
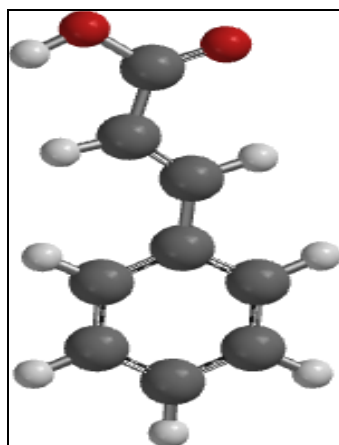


**Quercetin**

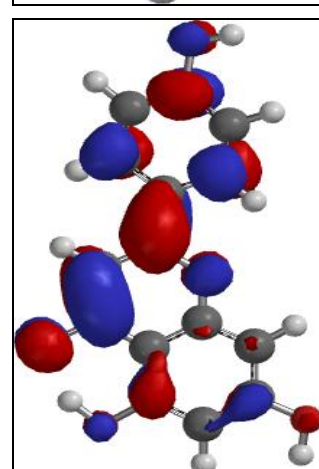
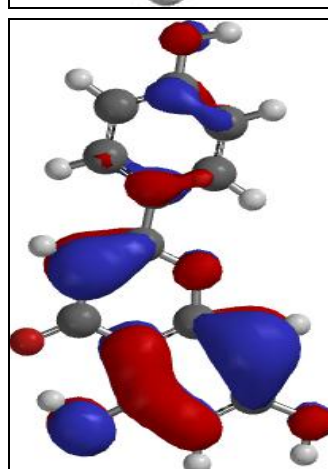
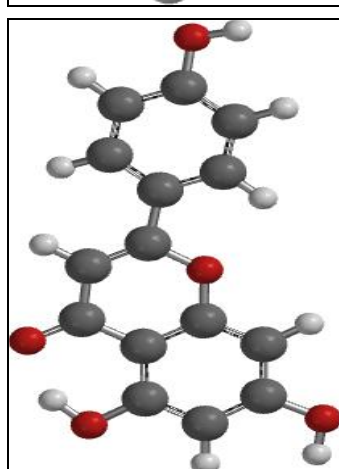




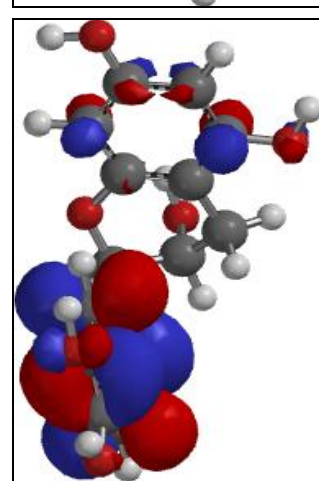
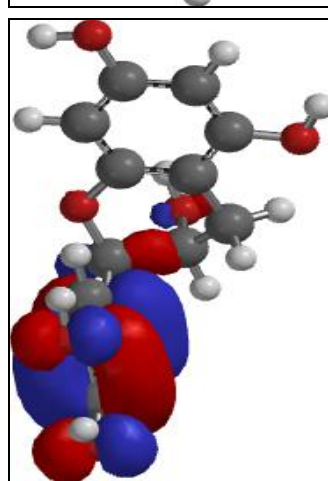
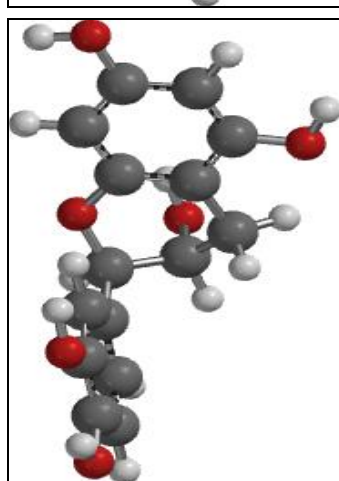
**Catechin**



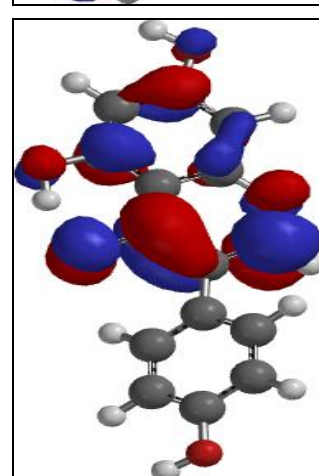
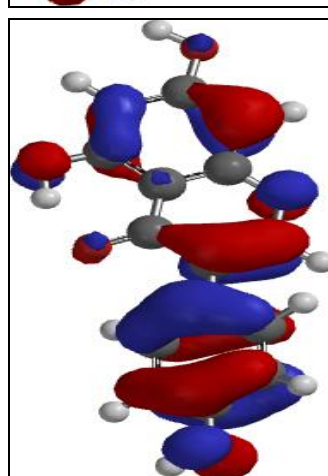
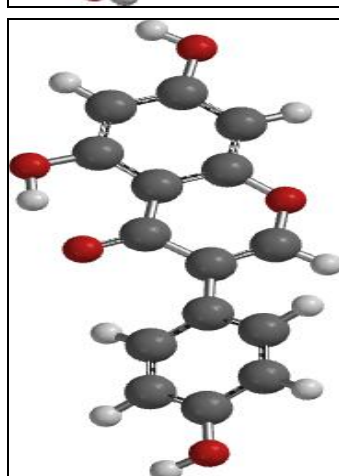
**Apigenin**



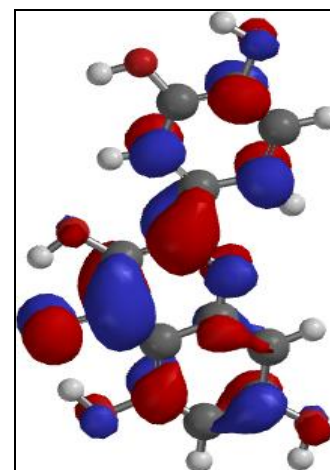
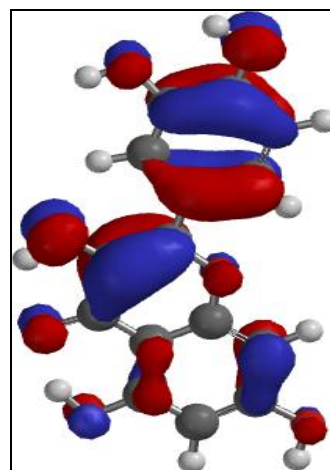
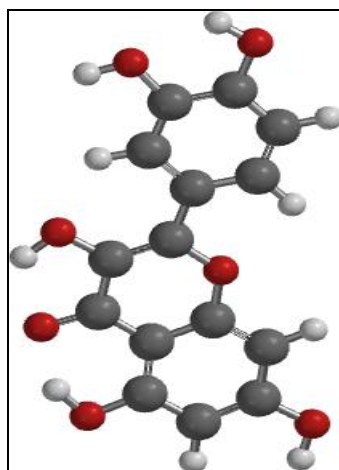
**Hesperetin**



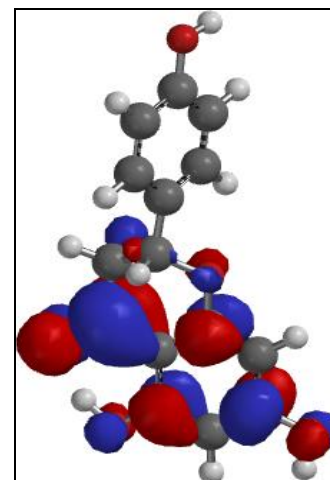
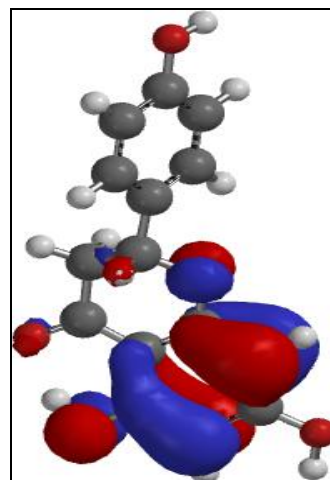
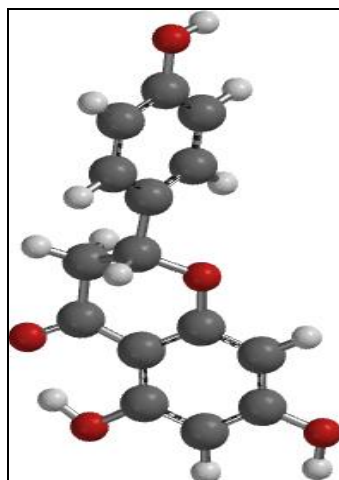
**Genistein**



**Kaempferol**



**Formononetin**



**FIG. 6 DFT RESULTS OF STRUCTURES OF THE LIGANDS IN OPTIMIZED, HOMO AND LUMO FORM**

**TABLE 5: THE CALCULATED THERMODYNAMIC QUANTITIES (ENTHALPY AND FREE ENERGY), VIA DFT FOR ALL PREDICTED INHIBITORS**

Compounds	$E_{HOMO}$ (eV)	$E_{LUMO}$ (eV)	$E_g$ (eV)	$I$ (eV)	$A$ (eV)	$\eta$ (eV)	$\delta$ (eV <sup>-1</sup> )	$\chi$ (eV)
Epigallocatechin gallate	-5.56	-1.01	4.55	5.56	1.01	2.275	0.43956	3.285
Myricetin	-6.63	-1.31	5.32	6.63	1.31	2.66	0.37594	3.97
Quercetin	-5.47	-1.84	3.63	5.47	1.84	1.815	0.550964	3.655
Catechin	-6.85	-1.94	4.91	6.85	1.94	2.455	0.407332	4.395
Apigenin	-5.91	-1.73	4.18	5.91	1.73	2.09	0.478469	3.82
Hesperetin	-5.63	0.08	5.71	5.63	-0.08	2.855	0.350263	2.775
Genistein	-5.7	-1.5	4.2	5.7	1.5	2.1	0.47619	3.6
Kaempferol	-5.48	-1.84	3.64	5.48	1.84	1.82	0.549451	3.66
Formononetin	-6.04	-1.43	4.61	6.04	1.43	2.305	0.433839	3.735

**TABLE 6: THIS INCLUDES THE GIBBS FREE ENERGY, ENTHALPY, MOLECULAR WEIGHT AND ELECTRONIC ENERGY**

Compounds	Molecular Weight (AMU)	Electronic Energy(AU)	Enthalpy (AU)	GIBBS Free Energy (Hartree)	Dipole Moment (Debye)
Epigallocatechin gallate	458.374	-1676.61	-1676.20	-1676.28	4.09
Myricetin	164.16	-573.42	-573.26	-573.30	6.37
Quercetin	318.24	-1179.39	-1179.14	-1179.20	1.51
Catechin	148.61	-498.21	-498.06	498.10	5.28
Apigenin	270.24	-953.74	-953.50	-953.56	5.05
Hesperetin	290.27	-1031.33	-1031.04	-1031.10	3.56
Genistein	270.24	-953.77	-953.50	-953.55	1.29
Kaempferol	302.238	-1104.18	-1103.93	-1103.99	0.22
Formononetin	272.26	-954.97	-954.68	-954.74	2.61

**DISCUSSION:** Cancerous cells have been shown to consume more biological fuel, which promotes their survival, growth, and multiplication. Since cancer cells produce GLUT4 at higher levels than normal cells do, inhibiting GLUT4 may have chemotherapy-like effects. This study used a computational screen to determine the binding affinity of several Phyto-ligands from Panax ginseng that have been claimed to have some anticancer properties. Overall, computer studies have reduced the possibility of a drug failing in the late stages of development.

**Docking / MMGBSA:** The compounds with the best MM/GBSA screening findings and docking scores are visually represented in **Fig. 4** and **3** and **Table 1**, respectively. **Fig. 5** displays the 2D and 3D structures of the hit compounds. In **Fig. 5**, the binding posture and interactions of hit compounds with the amino acid residues in the active site of 7WSN and the amino acid residues depicted in the interaction are analyzed as part of the post-docking analysis of the docking experiment. The ADME/Tox screening outcomes to predict the characteristics of the hit compounds' drug-likeness are also shown in **Tables 3** and **4**.

For their ability to inhibit the target protein GLUT4, the selected phytoligands from Panax ginseng were docked with enhanced precision (XP) in the protein's binding pocket. We examined the crucial amino-acid interactions in the GLUT4 binding region as well as the structural interactions between the top molecules<sup>31</sup>.

According to **Table 1**, the top ten ligands had docking scores ranging from -7.88 and -42.158 for Formononetin, the co-crystallized Cytochalasin B, and -6.635 and -48.971 for Epigallocatechin gallate, the lead chemical, with the lowest binding energy of -14.063kcal/mol and an MM-GBSA score of -34.471. Interactions are shown in detail in **Table 2**. MM-GBSA is used as a computational thermodynamics tool to evaluate the binding affinity of substances. Prior research has shown that the Prime module of the Schrodinger suite's MM-GBSA algorithm provides a reliable statistical post-docking analysis of docked complexes, with the lower the score, the higher the binding. Epigallocatechin gallate, Ginsenoside Rh 1, Myricetin, Catechin, Apigenin, Hesperitin,

Genistein, Kaempferol, and Formononetin all have relative free binding energies of -34.471, -59.497, -47.643, -51.274, -39.293, -35.795, -54.406, -40.813, -46.832, and -42.158 **Table 1**. Some of the bioactive compounds in issue had higher binding energy than the reference molecule, according to the MM-GBSA data (Cytochalasin B -48.971).

**ADME-Tox:** Bioavailability is the percentage of an unaltered medication that enters the systemic circulation after being administered via any method<sup>32</sup>. A substance is considered to have low oral bioavailability if its bioavailability score is lower than 0.5. If the score is more than 0.5, the substance is anticipated to have a high oral bioavailability. Using SWISS ADME, the bioavailability values of Epigallocatechin gallate, Ginsenoside Rh 1, Myricetin, Quercetin, Catechin, Apigenin, Hesperitin, Genistein, Kaempferol, and Formononetin range from 0.17 to 0.55, whereas Epigallocatechin gallate and Ginsenoside Rh 1 have a low bioavailability score of 0.17. This suggests that the majority of the phyto-ligands are likely candidates for use as medications.

As demonstrated in **Table 4**, additional toxicity indicators, including mutagenicity, hepatotoxicity, and carcinogenicity, were assessed and researched.

**Frontier Molecular Orbitals (FMOs):** The energies of the FMOs provide insight into the reactivity of the compounds. In contrast to the LUMO energy, which predicts how a molecule can take electrons, the HOMO energy describes how a molecule can donate electrons. Because they are crucial to the optical electric characteristics of molecules, the FMOs, LUMOs and HOMO orbitals are crucial in molecules. When molecules have high HOMO energy, they are more likely to give electrons, and when they have a low LUMO energy, they are more likely to take electrons, increasing their reactivity<sup>33</sup>. According to **Table 5**, the selected compounds' EHOMO values rise in the following order: Order With values ranging from 5.47 eV to 6.85 eV, the chemicals Catechin, Myricetin, Formononetin, Apigenin, Genistein, Hesperitin, Epigallocatechin gallate, Kaempferol, and Quercetin would likely interact through electron donation. This shows that cinnamic acid interacts more with other chemicals during chemical processes by donating electrons.



According to the ELUMO values, which range from 1.94 eV to - 0.08 eV, they would interact by taking in electrons. On the other hand, catechin interacts with chemical reactions more than other substances do by taking electrons. The band gap energy, which lies between the EHOMO and ELUMO and varies from 3.63 to 5.71eV, is crucial for determining the thermochemical reactivity of a molecule. The band gap energy values represent a molecule's chemical stability and reactivity. As the band gap energy rises, the molecule becomes tougher, more stable, and less reactive. A narrowing of the energy band gap indicates increased reactivity and decreased stability. A narrowing of the energy band gap indicates low stability and high reactivity. The values of the energy band gap rise in the following order: Formononetin, Catechin, Myricetin, Hesperetin, Kaempferol, Apigenin, Genistein, Epigallocatechin Gallate.

The global reactivity descriptor was used to determine the compounds' chemical hardness, softness, electronegativity, and chemical potential to verify their reactivity (GRD). Chemical hardness ( $\eta$ ) indicates how resistant a molecule is to the deformation of an electron cloud. In contrast to soft molecules, which are more easily polarizable and have a smaller band gap energy than hard molecules, hard molecules have a big energy band gap. The hardest compound was hesperetin, with a hardness value of 2.86 eV, while quercetin had the weakest value at 1.82 eV. All of the compounds under study had electro negativity values that fell within a specific range, with catechin (4.40 eV) having the highest. Electronegativity ( $\chi$ ) is the property of a molecule to attract electrons towards itself in a chemical reaction. In **Fig. 6**, the Optimized, HOMO and LUMO structures of the compound were shown. Electronic affinities for our projected inhibitors range from -0.08 to 1.94 eV. The capacity to create an anion is greatest in catechin. With a value of 6.85 eV, it has the highest potential for electron loss among all ionization energies. The calculated thermodynamic quantities (enthalpy and free energy), *via* DFT for all predicted inhibitors are presented in **Table 5** and **6** including their molecular weight.

**CONCLUSION:** According to reports, Panax ginseng has some anti-diabetic properties and may

one day be utilized to treat diabetes. Oyinloye's paper on the impact of GLUT4 antagonists on cancer cells was also included<sup>27</sup>. As a result, this study's computational analysis of some of Panax ginseng's anti-cancer phyto-ligands provided the foundation for its findings. The phyto-ligands' poor docking scores suggest that they have a high potential for inhibiting glucose transporter 4 activity. Compared to the co-crystallized molecule, ten bioactive components from Panax ginseng were found to have a high binding affinity for the target 7WSN (Cytochalasin B).

**Declaration:** None.

**Ethics Approval and Consent to Participate:** The study was approved by the Ethical unit of Molecular Biology and Simulation Center, Ado-Ekiti, Ekiti State, Nigeria, with a reference number of MSERB/CADD/ NHNAS/2022/07.

**Consent for Publication:** Not Applicable.

**Availability of Data and Material:** The data underlying this article are available in the article and its online supplementary material.

**Funding:** This research received no external funding.

**ACKNOWLEDGMENT:** We acknowledge the management of the research unit (*MOLS & SIMS*) for the provision of the needed facilities for this research work and the indefatigable Mrs. O. peyemi Y. Omotuyi (PPh.D. for her steady support and care.

**CONFLICT OF INTEREST:** The authors declare that there is no conflict of interest regarding the publication of this paper.

#### REFERENCES:

1. World Health Organization Cancer. Available online: <https://www.who.int/news-room/fact-sheets/detail/cancer> (accessed on 8 August 2021).
2. Chester M. Southam. The Complex Etiology of Cancer. Cancer Research. Downloaded from [http://aacrjournals.org/cancerres/article-pdf/23/8\\_Part\\_1/1105/2378743/cr0238p11105.pdf](http://aacrjournals.org/cancerres/article-pdf/23/8_Part_1/1105/2378743/cr0238p11105.pdf) by guest on 18 July 2022.
3. Monjotin N, Amiot MJ, Fleurentin J, Morel JM and Raynal S: Clinical Evidence of the Benefits of Phytonutrients in Human Healthcare. *Nutrients* 2022; 14(9): 1712. <https://doi.org/10.3390/nu14091712>
4. Haslam A. Robb, Hébert SW, Huang JR and Ebell HMM: Association between dietary pattern scores and the

- prevalence of colorectal adenoma considering population subgroups. *Nutr Diet* 2018; 75: 167–175. [CrossRef]
5. Mehta RS, Song M, Nishihara R, Drew DA, Wu K, Qian ZR, Fung TT, Hamada T, Masugi Y and da Silva A: Dietary Patterns and Risk of Colorectal Cancer: Analysis by Tumor Location and Molecular Subtypes. *Gastroenterology* 2017; 152: 1944–1953.e1. [CrossRef] [PubMed]
  6. Kamal N, Ilowefah MA, Hilles AR, Anua NA, Awini T, Alshweyh HA, Aldosary SK, Jambocus NGS, Alosaimi AA and Rahman A: Genesis and mechanism of some cancer types and an overview on the role of diet and nutrition in cancer prevention. *Molecules* 2022; 27: 1794. <https://doi.org/10.3390/molecules27061794>
  7. Buendia Jimenez I, Richardot P, Picard P, Lepicard EM, De Meo M and Talaska G: Effect of Increased Water Intake on Urinary DNA Adduct Levels and Mutagenicity in Smokers: A Randomized Study. *Dis Markers* 2015; 2015: 478150. [CrossRef]
  8. Wang J, Wu X, Kamat A, Barton Grossman H, Dinney CP and Lin J: Fluid intake, genetic variants of UDP-glucuronosyltransferases, and bladder cancer risk. *Br. J. Cancer* 2013; 108: 2372–2380. [CrossRef] [PubMed]
  9. Dobruch J and Oszczudłowski M: Bladder Cancer: Current Challenges and Future Directions. *Medicina (Kaunas)*. 2021; 57(8): 749. doi: 10.3390/medicina57080749. PMID: 34440955; PMCID: PMC8402079.
  10. Wierzejska R: Coffee consumption vs. cancer risk—a review of scientific data. *Rocz Panstw Zakl Hig* 2015; 66: 293–298. [PubMed]
  11. Hajjar M, Rezazadeh A, Naja F, Kardoust Parizi M, Alaghebandan R, Pourkerman M & Rashidkhani B: Association of recommended and non-recommended food score and risk of bladder cancer: A case-control study. *Nutrition and Cancer* 2022; 74(6): 2105–2112.
  12. Kassam S and Freeman L: The Role of Nutrition in Cancer Prevention - Should You Listen to Your Doctor or Influencer? *American Journal of Lifestyle Medicine*. 2022; 0(0). doi:10.1177/15598276221112331
  13. Liu H, Wang XC, Hu GH, Guo ZF, Lai P, Xu L, Huang TB and Xu YF: Fruit and vegetable consumption and risk of bladder cancer: An updated meta-analysis of observational studies. *Eur J Cancer Prev* 2015; 24: 508–516. [CrossRef]
  14. Zhao YM, Wang XP, Jin KY, Dong DJ, Reiff T & Zhao XF: Insulin-like Growth Factor 2 Promotes Tissue-Specific Cell Growth, Proliferation and Survival during Development of *Helicoverpa armigera*. *Cells* 2022; 11(11): 1799.
  15. Fuming Zi, Huapu Zi, Yi Li, Jingsong He, Qingzhi Shi, and Zhen CA: Metformin and cancer: An existing drug for cancer prevention and therapy (Review). *Oncology Letters* 2018; 15: 683–690. DOI: 10.3892/ol.2017.7412
  16. Nisha Y, Dubashi B, Bobby Z, Sahoo JP & Kayal S: Effect of cytotoxic chemotherapy on bone health among breast cancer patients. Does it require intervention. *Supportive Care in Cancer* 2021; 29(11): 6957–6972.
  17. Yamazaki CM, Yamaguchi A, Anami Y, Xiong W, Otani Y, Lee J & Tsuchikama K: Antibody-drug conjugates with dual payloads for combating breast tumor heterogeneity and drug resistance. *Nature Communications* 2021; 2(1): 1–13.
  18. Salem DS, Hegazy SF & Obayya SS: Nanogold-loaded chitosan nanocomposites for pH/light-responsive drug release and synergistic chemo-photothermal cancer therapy. *Colloid and Interface Science Communications* 2021; 41: 100361.
  19. Mohamed Yafout, Amine Ousaid, Youssef Khayati and Ibrahim Sbai El Otmani: Gold nanoparticles as a drug delivery system for standard chemotherapeutics: A new lead for targeted pharmacological cancer treatments. *Scientific African* 11 2021; e00685. <https://doi.org/10.1016/j.sciaf.2020.e00685>.
  20. Smorodina E, Tao F, Qing R, Jin D, Yang S & Zhang S: Comparing 2 crystal structures and 12 AlphaFold2-predicted human membrane glucose transporters and their water-soluble glutamine, threonine, and tyrosine variants. *QRB Discovery* 2022; 3.
  21. Krishna TP, Maharajan T & Ceasar SA: The role of membrane transporters in the biofortification of zinc and iron in plants. *Biological Trace Element Res* 2022; 1–15.
  22. Changyong Wei, Richa Bajpai, Horrick Sharma, Monique Heitmeier, Atul D. Jain, Shannon M. Matulis, Ajay K. Nooka, Rama K. M Mishra, Paul W. Hruz, Gary E. Schiltz and Mala Shanmugam: Development of GLUT4-selective antagonists for multiple myeloma therapy. *Eur J Med Chem* 2017; 139: 573–586. doi:10.1016/j.ejmech.2017.08.029.
  23. Kjøbsted R & Wojtaszewski JF: Comment on de Wendt et al. Contraction-mediated glucose transport in skeletal muscle is regulated by a framework of AMPK, TBC1D1/4, and Rac1. *Diabetes* 2021; 70: 2796–2809. *Diabetes*, 71(3), e3–e4.
  24. Lopez-Lazaro M: Does hypoxia control tumor growth? *Cell Oncol* 2006; 28: 327–329.
  25. Lopez-Lazaro M: Why do tumors metastasize? *Cancer Biol Ther* 2007; 6: 141–144.
  26. Gatenby RA, Gawlinski ET, Gmitro AF, Kaylor B and Gillies RJ: Acid-mediated tumor invasion: a multidisciplinary study. *Cancer Res* 2006; 66: 5216–5223.
  27. Babatunji Emmanuel Oyinloye, Tayo Alex Adekiya, Raphael Taiwo Aruleba, Oluwafemi Adeleke Ojo and Basiru Olaitan Ajiboye: Structure Based Docking Studies of GLUT4 towards Exploring Selected Phytochemicals from *Solanum Xanthocarpum* as a Therapeutic target for the Treatment of Cancer. *Current Drug Discovery Technology* 2019.
  28. Wang N: Ginseng polysaccharides: A potential neuroprotective agent. *Journal of Ginseng Research*, <https://doi.org/10.1016/j.jgr.2020.09.002>
  29. Raposo, Antonio, Saraiva, Ariana, Ramos, Fernando, Carrascosa, Conrado, Raheem, Dele, Bárbara, Rita, Silva and Henrique: The Role of Food Supplementation in Microcirculation. A Comprehensive Review. *Biology* 2021; 10: 616. 10.3390/biology1007061
  30. Qi Ls W, Wang CZ and Yuan CS: Ginsenosides from American ginseng: Chemical and pharmacological diversity. *Phytochemistry* 2011; 72: 689–699.
  31. Olugbogi EA, Bodun DS, Omoseye SD, Onoriode AO, Oluwamototi FO, Adedara JF & Omotuyi OI: Quassia amara bioactive compounds as a Novel DPP-IV inhibitor: an *in-silico* study. *Bulletin of the National Research Centre* 2022; 46(1): 1–14.
  32. Kim S, Thiessen PA, Bolton EE, Chen J, Fu G, Gindulyte A & Wang J: BS The PubChem Project. *Nucleic Acids Research* 2016; 44(1): 1202–13.
  33. Damilola A. Omoboyowa, Muhammad N. Iqbal, Toheeb A. Balogun, Damilola S. Bodun, John O. Fatoki and Oluwatoba E. Oyeneyin: Inhibitory potential of phytochemicals from *Chromolaena odorata* L. against apoptosis signal-regulatory kinase 1: A computational model against colorectal cancer, *Computational Toxicology* 2022; 23: 100235, ISSN 2468-1113, <https://doi.org/10.1016/j.comtox.2022.100235>.

**How to cite this article:**

Olugbogi EA, Omotuyi OI, Mesileya KT, Bodun DS, Omoseeye SD, Onoriode AO, Oluwamoroti FO, Adedara JF, Oriyomi IA, Bello FO, Olowoyeye FO, Laoye OG, Adebawale DB, Adebisi AD, Ogologo MC, Etukokwu OC, Onyemaobi IO, Jibril SY and Onyeka PC: Computer based screening of the anticancer property of selected panax ginseng phyto-ligands. Int J Pharm Sci & Res 2023; 14(4): 1714-27. doi: 10.13040/IJPSR.0975-8232.14(4).1714-27.

All © 2023 are reserved by International Journal of Pharmaceutical Sciences and Research. This Journal licensed under a Creative Commons Attribution-NonCommercial-ShareAlike 3.0 Unported License.

This article can be downloaded to **Android OS** based mobile. Scan QR Code using Code/Bar Scanner from your mobile. (Scanners are available on Google Playstore)